Supporting Information for

Zn-Sn interface layer design strategy towards high-stability Zn powder anode

Yan Xin[1], Yunnian Ge[1], Ming Lei[1], Shen Cai[1], Chen Zhao[1], Huai Zhang[2] and Huajun Tian[1*]*

Y. Xin, Y. Ge, M. Lei, S. Cai, C. Zhao, H. Tian

[1] Beijing Laboratory of New Energy Storage Technology and Key Laboratory of Power Station Energy Transfer Conversion and System of Ministry of Education, School of Energy Power and Mechanical Engineering, North China Electric Power University, Beijing, 102206, China

E-mail: Huajun.Tian@ncepu.edu.cn

H. Zhang

[2] Wuhu Churui Intelligent Technology Co., Ltd, Wuhu, 241002, China

E-mail: huai.zhang@whcrit.com

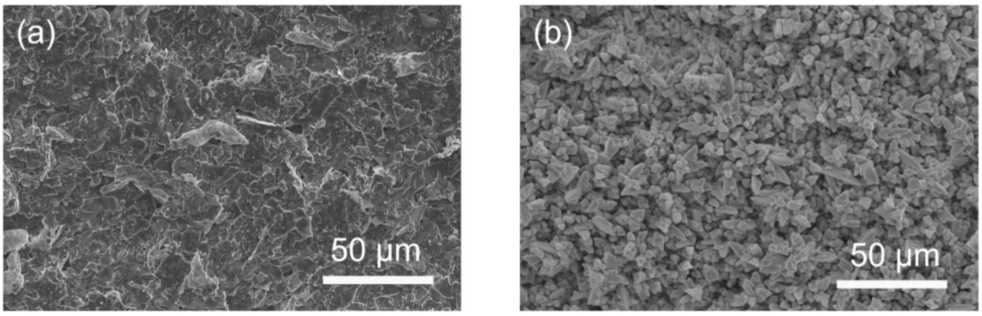

Figure S1. (a) SEM images of (a) Zn powder and (b) ZnSn@ZP anodes.

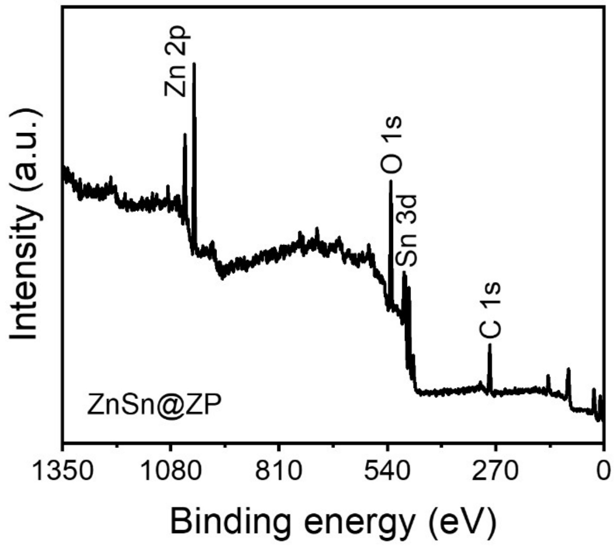

Figure S2. Full XPS spectra of ZnSn@ZP anode.

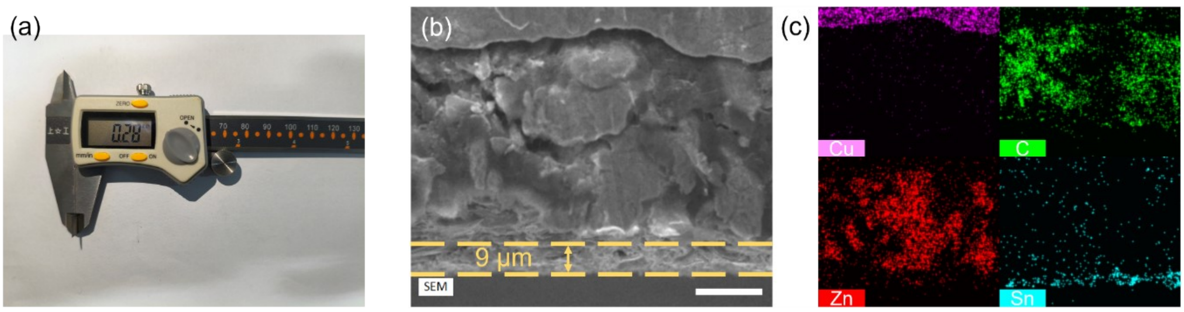

Figure S3. (a) Thickness observation of Zn powder anode. (b) Cross-sectional SEM image of ZnSn@ZP anode. Scale bar: 20 μm. (c) The cross-sectional EDS elemental mappings of ZnSn@ZP anode.

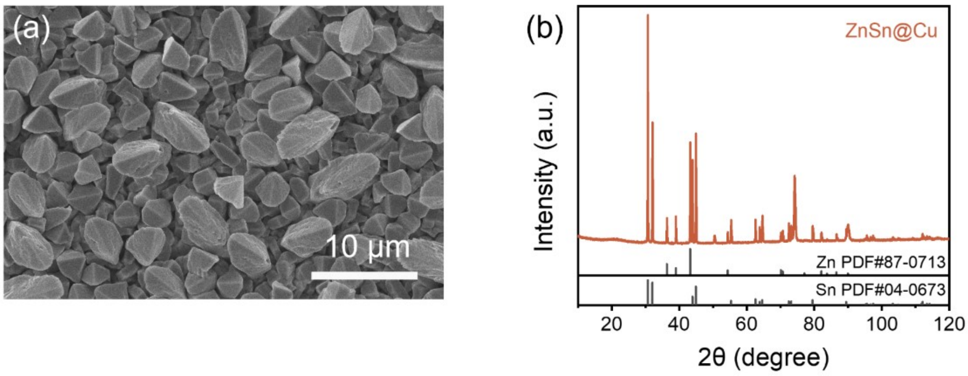

Figure S4. (a) SEM image and (b) XRD pattern of ZnSn@Cu anode.

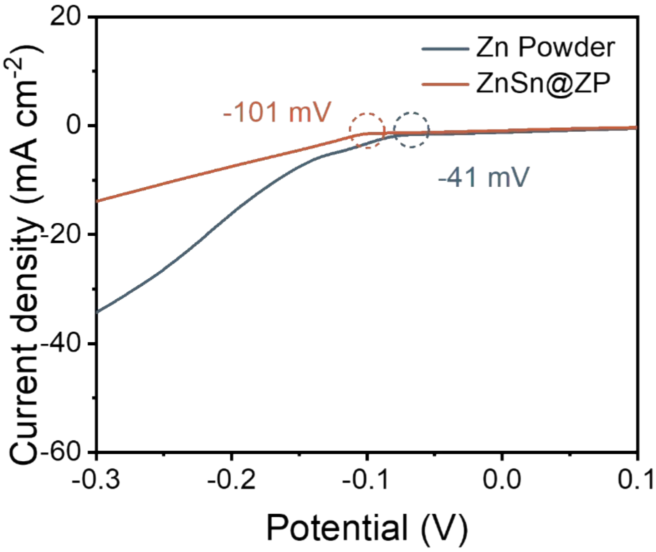

Figure S5. Hydrogen evolution analyzed by LSV curves of Zn powder and ZnSn@ZP anodes (stainless steel foil as working electrode, two anodes as counter and reference electrode).

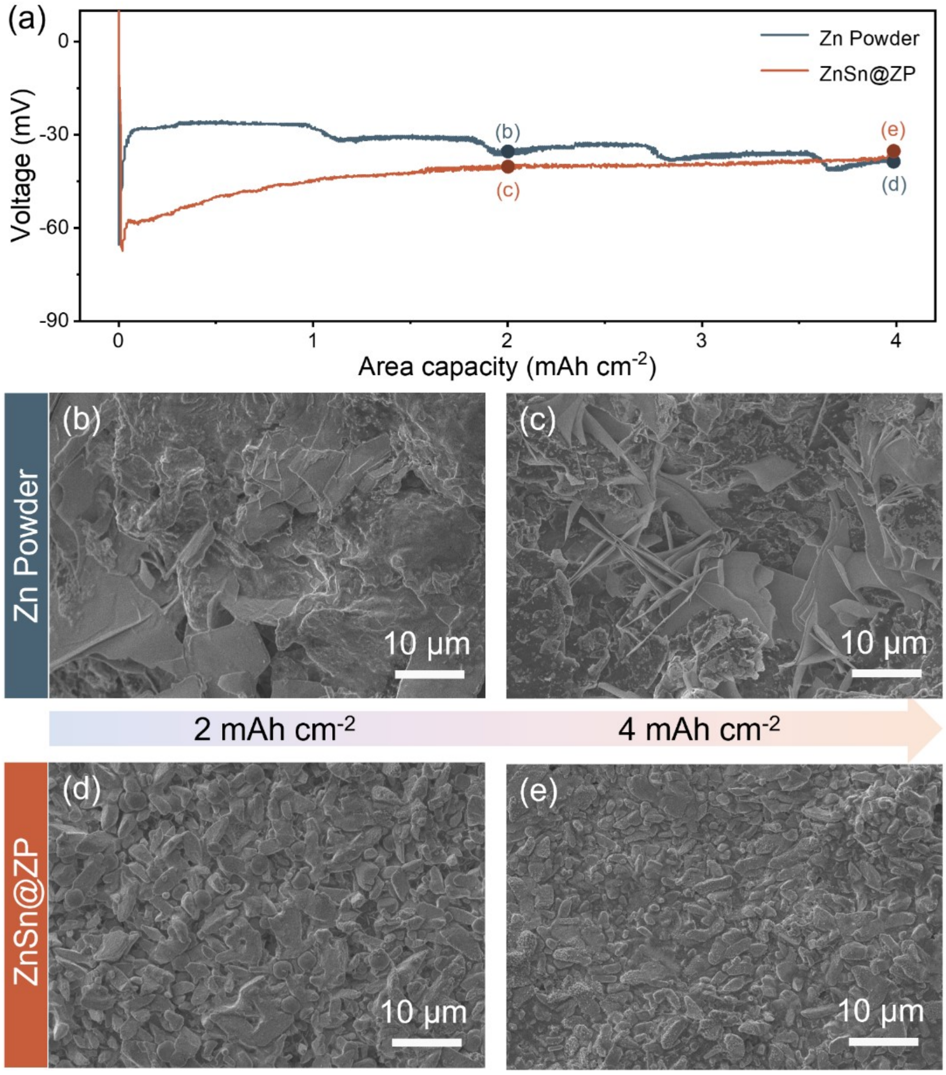

Figure S6. (a) The initial Zn deposition voltage profiles of the Zn powder and ZnSn@ZP anodes at 1 mA cm^{-2}. Morphology evolution of (b-c) Zn powder and (d-e) ZnSn@ZP anodes with a plating areal capacity from 2 mAh cm^{-2} to 4 mAh cm^{-2}.

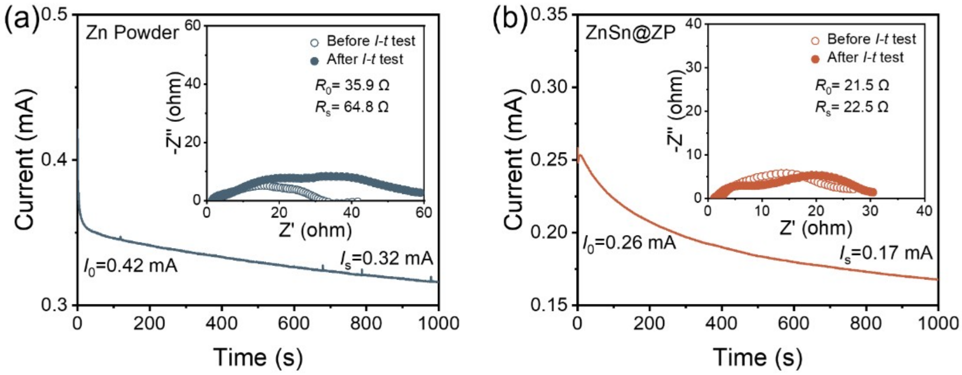

Figure S7. *I-t* plots of symmetric cells based on (a) Zn powder and (b) ZnSn@ZP anodes after the application of a constant potential (10 mV). The insets show the EIS results for symmetric cells before and following polarization (*I-t* test).

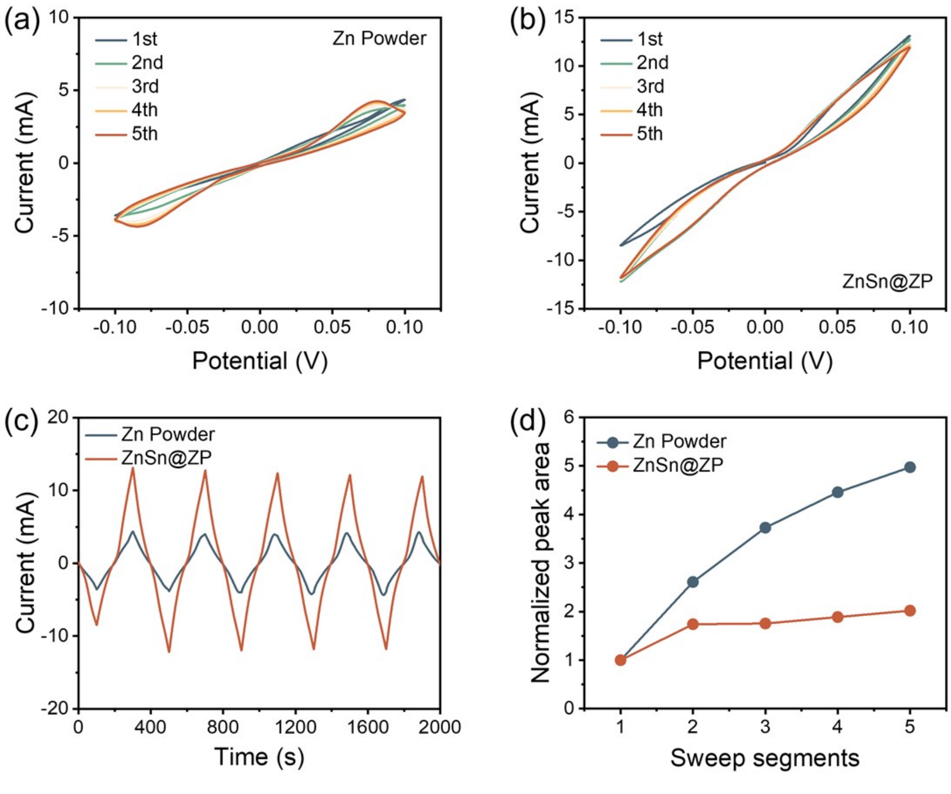

Figure S8. CV curves of the symmetric cells based on (a) Zn powder and (b) ZnSn@ZP anodes for the initial five cycles. (c) Current-Time profiles derived from CV curves. (d) Peak areas in CV curves.

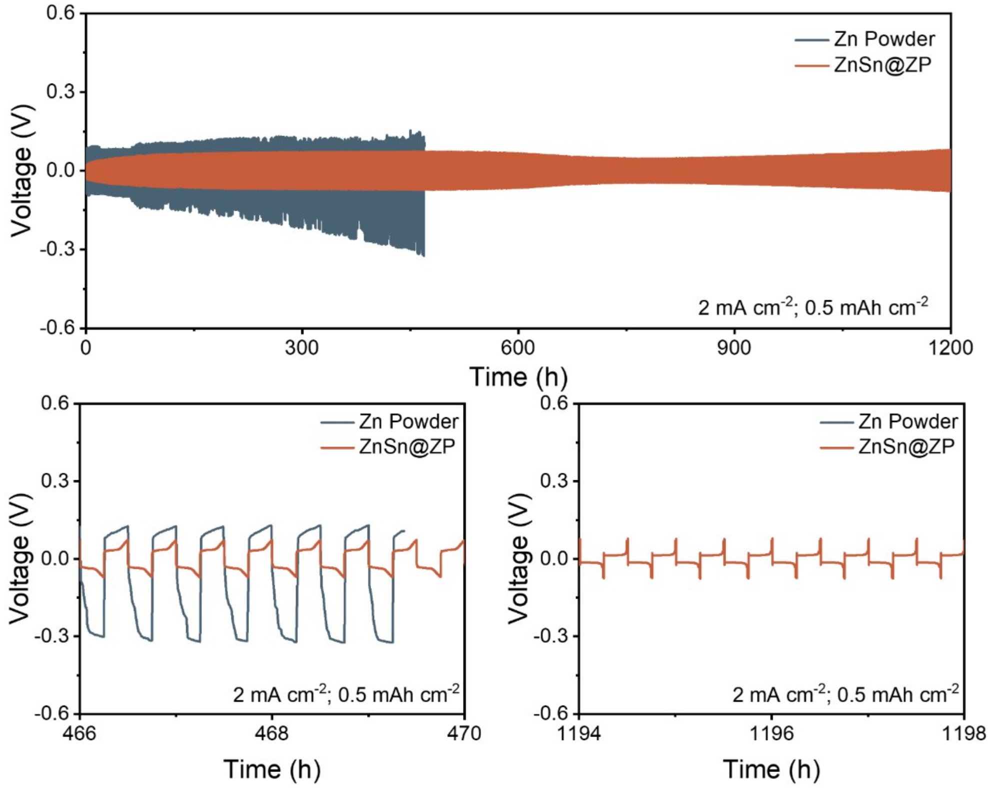

Figure S9. Cycling performance of symmetric cells based on Zn powder and ZnSn@ZP anodes at 2 mA cm^{-2} with areal capacity of 0.5 mAh cm^{-2}.

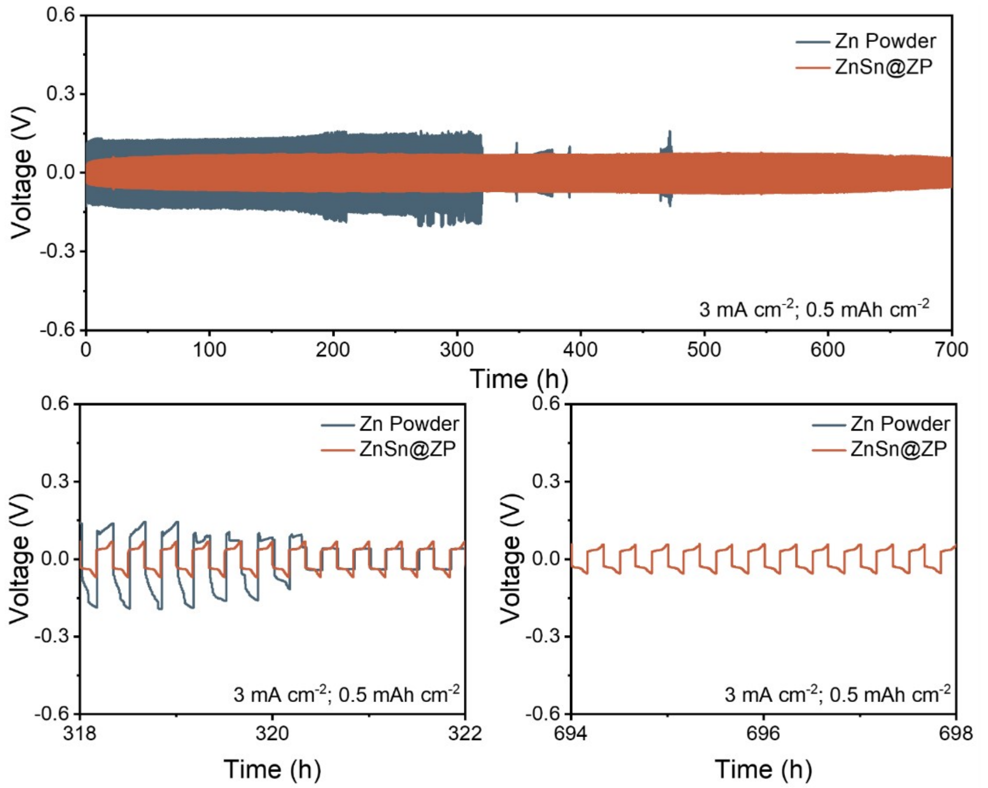

Figure S10. Cycling performance of symmetric cells based on Zn powder and ZnSn@ZP anodes at 3 mA cm^{-2} with areal capacity of 0.5 mAh cm^{-2}.

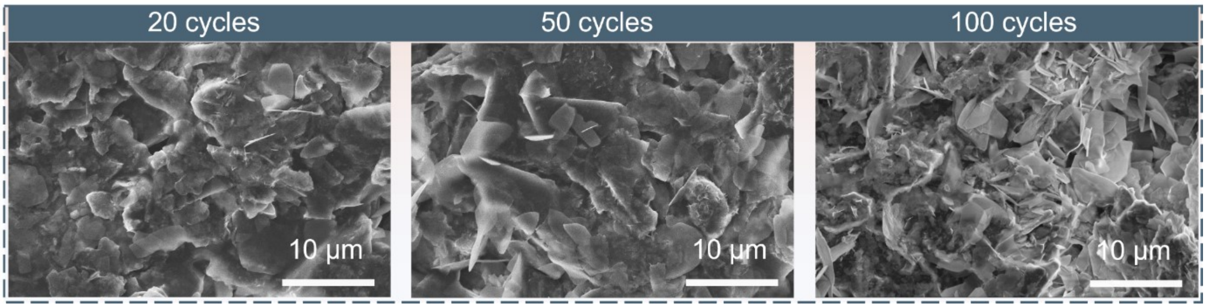

Figure S11. SEM images of symmetric cells based on Zn powder anode after 20, 50, 100 cycles.

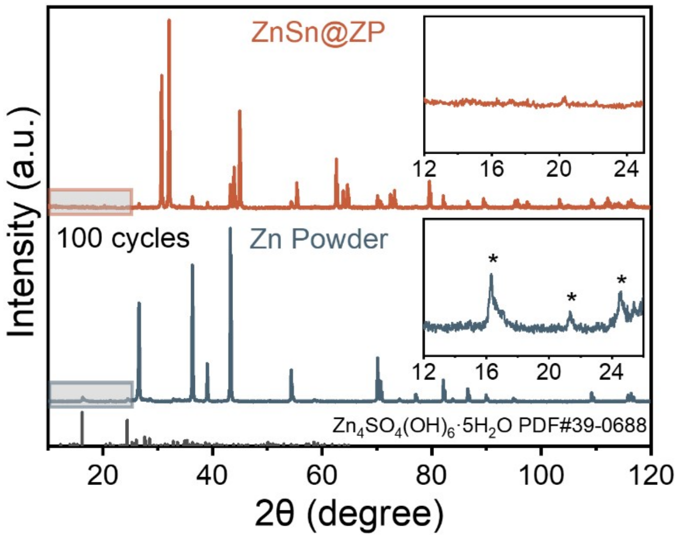

Figure S12. XRD patterns of symmetric cells based on Zn powder and ZnSn@ZP anodes after 100 cycles.

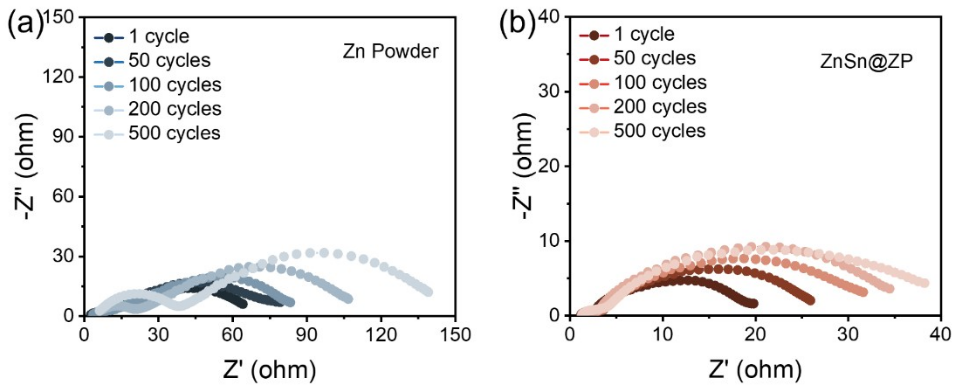

Figure S13. Nyquist plots of symmetric cells based on (a) Zn powder and (b) ZnSn@ZP anodes after different cycles at 1 mA cm^{-2} with areal capacity of 0.25 mAh cm^{-2}.

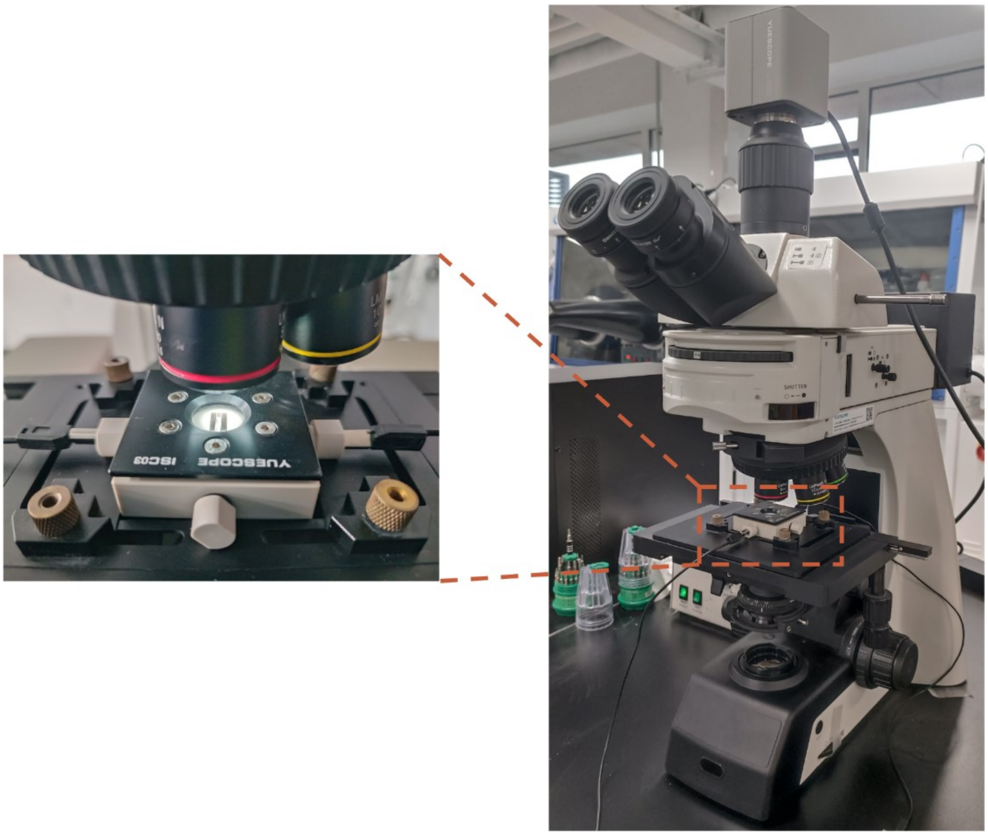

Figure S14. The device pictures for in situ optical observation.

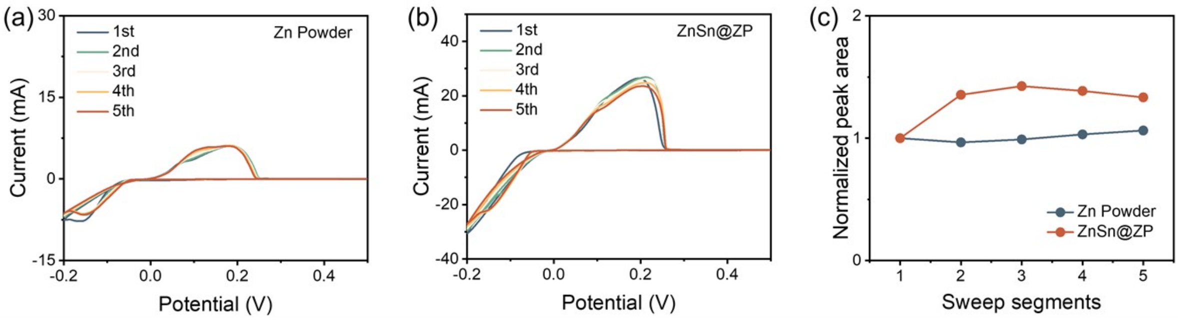

Figure S15. CV curves of asymmetric cells based on (a) Zn powder and (b) ZnSn@ZP anodes for the initial five cycles, and (c) corresponding peak areas.

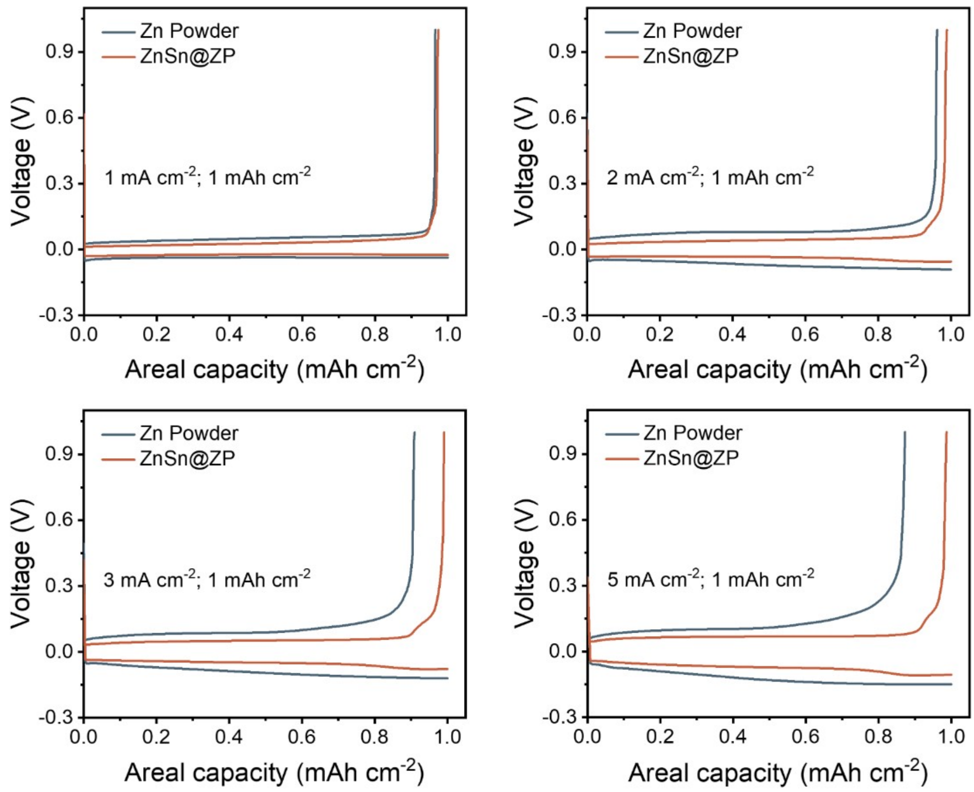

Figure S16. Charge-discharge voltage profiles of asymmetric cells based on Zn powder and ZnSn@ZP anodes at various current density ranges of 1-5 mA cm^{-2} with a fixed capacity of 1 mAh cm^{-2}.

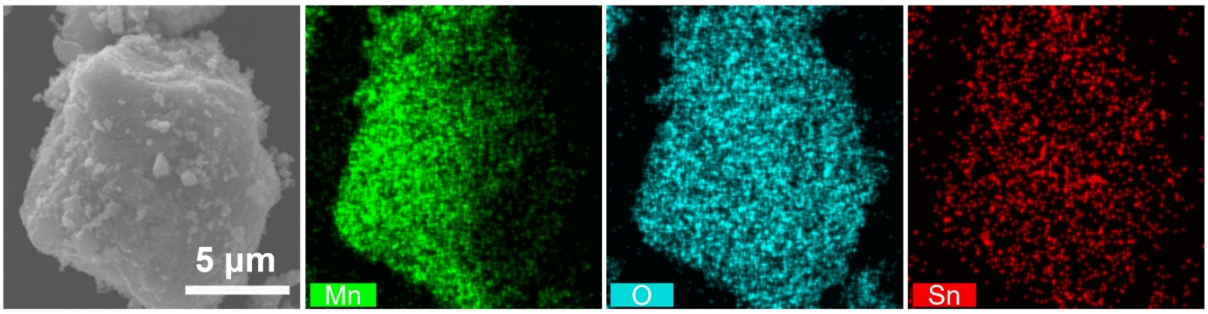

Figure S17. EDS elemental mappings of Sn-doped MnO_2.

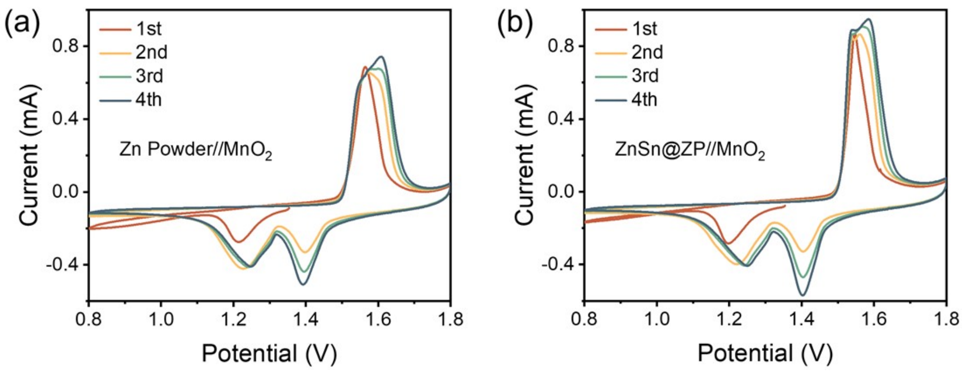

Figure S18. CV curves of (a) Zn powder//MnO_2 and (b) ZnSn@ZP//MnO_2 full cells for the initial four cycles at 0.2 mV s^{-1}.

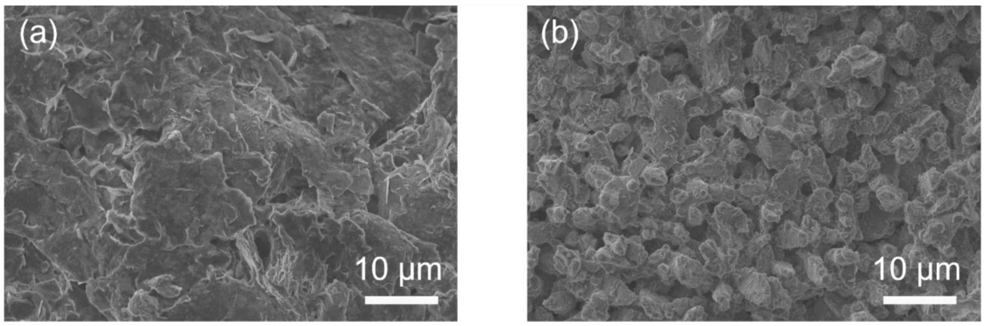

Figure S19. SEM images of the anodes in (a) Zn powder//MnO_2 and (b) ZnSn@ZP//MnO_2 full cells after 100 cycles at 1 A g^{-1}.

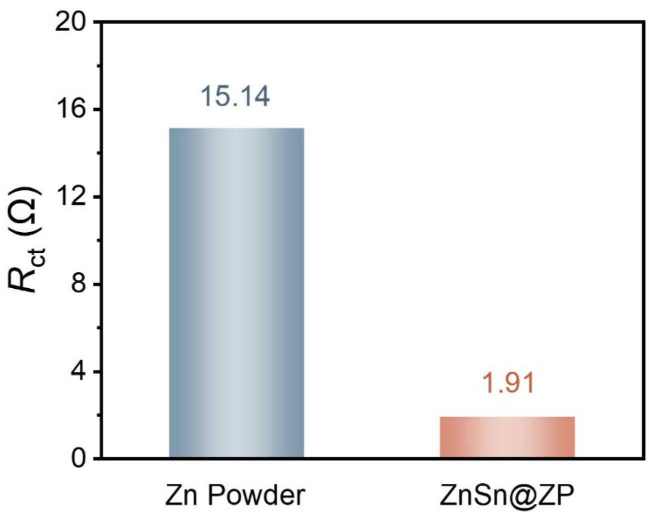

Figure S20. The fitting resistance results of the Zn powder//MnO_2 and ZnSn@ZP//MnO_2 full cells before cycling.

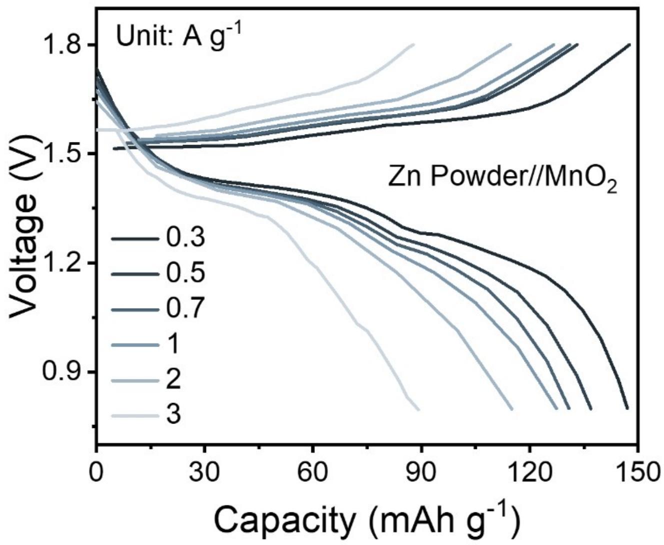

Figure S21 GCD curves of Zn powder//MnO_2 full cell.

Table S1. The fitting resistance results of symmetric cells based on Zn powder and ZnSn@ZP anodes before cycling.

Anodes	R_{ct} (Ω)
Zn Powder	58.46
ZnSn@ZP	18.44

Table S2. Performance comparison of symmetric cells based on ZnSn@ZP anode in this work and other previously reported Zn powder anodes.

Zn powder anode	Current density (mA cm^{-2})	Capacity (mAh cm^{-2})	Cycle life (h)	Voltage hysteresis (mV)	Refs
MXene@Zn	1	0.5	200	30	1
Zn powder/PG	1	1	400	51	2
Zn-P-MIEC	0.25	0.05	1300	83	3
Zn_rGO	1	1	550	20	4
3DP-ZA	1	1	320	35	5
SLA	2	2	490	~70	6
ZP-Grad	1	1	1250	25	7
SS-ZnP	1	1	400	~40	8
2D-Zn	2	1	90	~25	9
Zn-P@In	1	0.5	1000	121	10
M3DP-MXene/Cu-THBQ/Zn-P	2	1	1800	~100	11
PF@Zn	1	1	120	~30	12
Zn-PD3	1	1	240	~100	13
Zn@C-5	1	1	880	32	14
C@Zn-P	1	0.5	600	20	15
CuO@Zn	1	1	900	~20	16
A-Zn@CNTs	1	1	800	~74	17
Bi-MX@ZnP	0.5	0.5	250	20	18
ZnSn@ZP	1	0.25	1500	16	This work
ZnSn@ZP	2	0.5	1200	27	

Table S3. Performance comparison of symmetric cells based on ZnSn@ZP anode in this work and zinc foil anode based on COF/MOF/SnO_2 interface modification.

Zn anode	Current density (mA cm^{-2})	Capacity (mAh cm^{-2})	Cycle life (h)	Voltage hysteresis (mV)	Refs
PVDF@COF@Zn	1	1	600	53	19
Tp-Bpy@Zn	1	1	900	74.3	20
Zn-TFTDA COF	0.5	0.5	900	-	21
Zn@COF-S-F	1.5	0.75	1000	50.5	22
Zn@ZCM	1	1	2275	-	23
Zn//F-MOF	1	0.5	2000	49	24
Cu-TCPP@Zn	1	1	1400	23	25
MOF-5 W@Zn	1	1	600	~30	26
CDs/SnO_2-1@Zn	2	1	1100	~50	27
SnO_2@Zn	0.25	0.2	300	10	28
ZnSn@ZP	1	0.25	1500	16	This work
ZnSn@ZP	2	0.5	1200	27	

References

1. Li, X. L.; Li, Q.; Hou, Y.; Yang, Q.; Chen, Z.; Huang, Z. D.; Liang, G. J.; Zhao, Y. W.; Ma, L. T.; Li, M. A.; Huang, Q.; Zhi, C. Y., Toward a Practical Zn Powder Anode: $Ti_3C_2T_x$ MXene as a Lattice-Match Electrons/Ions Redistributor. *ACS Nano* **2021,** *15* (9), 14631-14642.
2. Du, W. C.; Huang, S.; Zhang, Y. F.; Ye, M. H.; Li, C. C., Enable commercial Zinc powders for dendrite-free Zinc anode with improved utilization rate by pristine graphene hybridization. *Energy Storage Materials* **2022,** *45*, 465-473.
3. Zhang, M.; Yu, P. F.; Xiong, K. R.; Wang, Y. Y.; Liu, Y. L.; Liang, Y. R., Construction of Mixed Ionic-Electronic Conducting Scaffolds in Zn Powder: A Scalable Route to Dendrite-Free and Flexible Zn Anodes. *Advanced Materials* **2022,** *34* (19), 2200860.
4. Lin, Y. H.; Hu, Y. Z.; Zhang, S.; Xu, Z. Q.; Feng, T. T.; Zhou, H. P.; Wu, M. Q., Binder-Free Freestanding 3D Zn-Graphene Anode Induced from Commercial Zinc Powders and Graphene Oxide for Zinc Ion Battery with High Utilization Rate. *ACS Applied Energy Materials* **2022,** *5* (12), 15222-15232.
5. Zeng, L.; He, J.; Yang, C. Y.; Luo, D.; Yu, H. B.; He, H. N.; Zhang, C. H., Direct 3D printing of stress-released Zn powder anodes toward flexible dendrite-free Zn batteries. *Energy Storage Materials* **2023,** *54*, 469-477.
6. Liu, Q.; Yu, Z. L.; Zhou, R.; Zhang, B., A Semi-Liquid Electrode toward Stable Zn Powder Anode. *Advanced Functional Materials* **2023,** *33* (5), 2210290.
7. Zhao, X.; Gao, Y.; Cao, Q. H.; Bu, F.; Pu, J.; Wang, Y. X.; Guan, C., A High-Capacity Gradient Zn Powder Anode for Flexible Zn-Ion Batteries. *Advanced Energy Materials* **2023,** *13* (38), 2301741.
8. Cao, C. H.; Zhou, K. Q.; Du, W. C.; Li, C. C.; Ye, M. H.; Zhang, Y. F.; Tang, Y. C.; Liu, X. Q., Designing Soft Solid-like Viscoelastic Zinc Powder Anode toward High-Performance Aqueous Zinc-Ion Batteries. *Advanced Energy Materials* **2023,** *13* (38), 2301835.
9. Cao, P. H.; Meng, Q.; Li, C. C.; Ran, L.; Zhou, X. Y.; Tang, J. J.; Bai, Q. X.; Yang, J., Dimensionality Reduction Engineering to Construct a Highly Stable Zn Powder Anode in Aqueous Zn-Ion Batteries. *ACS Applied Energy Materials* **2023,** *7* (2), 479-486.
10. Li, A. X.; Chen, M. F.; Tian, Q. H.; Han, X.; Chen, J. Z., Conquering poor reversibility of zinc powder electrode through in-situ surface engineering towards long-life zinc-ion batteries. *Journal of Alloys and Compounds* **2023,** *965* (25), 171337.
11. Lu, H. Y.; Hu, J. S.; Zhang, K. Q.; Zhao, J. X.; Deng, S. Z.; Li, Y. J.; Xu, B. A.; Pang, H., Microfluidic-Assisted 3D Printing Zinc Powder Anode with 2D Conductive MOF/MXene Heterostructures for High-Stable Zinc-Organic Battery. *Advanced Materials* **2024,** *36* (6), 2309753.
12. Sha, L.; Sui, B. B.; Wang, P. F.; Gong, Z.; Zhang, Y. H.; Wu, Y. H.; Zhao, L. N.; Tang, J. J.; Shi, F. N., 3D network of zinc powder woven into fibre filaments for dendrite-free zinc battery anodes. *Chemical Engineering Journal* **2024,** *481*, 148393.
13. Li, Q.; Tang, S. H.; Luo, R. Y.; Wei, P.; Chen, P.; Cong, J. L.; Liu, G. Z.; Liu, Z. F.; Gou, Y. Z.; Wu, H. Z.; Sun, S. X.; Han, J. T.; Shi, Y. S.; Fang, C.; Yan, C. Z., Regulating the local chemical environment of Zn powder surface by multi-site anchoring effect to achieve highly-stable Zn anode. *Energy Storage Materials* **2024,** *66*, 103229.
14. Wang, J. X.; Zhang, H.; Yang, L. Z.; Zhang, S. Y.; Han, X. P.; Hu, W. B., In situ Implanting 3D Carbon Network Reinforced Zinc Composite by Powder Metallurgy for Highly Reversible Zn-based Battery Anodes. *Angewandte Chemie International Edition* **2024,** *63* (10), e202318149.
15. Tang, J. H.; Cao, J. L.; Jiang, Y. X.; Gou, S. Y.; Yao, R. Q.; Li, Y. Q.; Liu, B. T., Spraying amorphous carbon coated zinc to prepare powder-based anodes for long-life zinc-ion batteries. *Green Chemistry*

2024, *26* (13), 7990-7996.
16. Liu, G. Q.; Fu, B.; Liu, Z. X.; Li, L. Y.; Liang, S. Q.; Fang, G. Z., Copper oxide-modified highly reversible Zn powder anode for aqueous Zn metal batteries. *Rare Metals* **2024,** *43* (10), 5005-5016.
17. Shao, Y. Y.; Xia, Z.; Xu, L.; Zhang, X. Y.; Yang, D. Z.; Yang, Z. C.; Luo, J. R.; Xiao, G.; Yang, Y. N.; Su, Y. W.; Lu, G. Q.; Sun, J. Y.; Cheng, T.; Shao, Y. L., Crystalline Texture Reengineering of Zinc Powder-Based Fibrous Anode for Remarkable Mechano-Electrochemical Stability. *Advanced Materials* **2024,** *36* (40), 2407143.
18. Yang, Z. X.; Wang, Z. Y.; Cao, J. L.; Wang, S. N.; Lei, W. W.; Wang, X. A.; Liu, D., Stabilizing zinc powder anodes via bifunctional MXene towards flexible zinc-ion batteries. *Journal of Colloid and Interface Science* **2025,** *680*, 657-664.
19. Aupama, V.; Sangsawang, J.; Kao-ian, W.; Wannapaiboon, S.; Pimoei, J.; yoopensuk, W.; Opchoei, M.; Tehrani, Z.; Margadonna, S.; Kheawhom, S., Adaptive COF-PVDF composite artificial solid electrolyte interphase for stable aqueous zinc batteries. *Electrochimica Acta* **2024,** *506*, 145059.
20. Liang, L. P.; Su, L.; Zhang, X.; Wang, Y. Q.; Ren, W. R.; Gao, X. P.; Zheng, L. Q.; Lu, F., Synergistically regulating Zn-ion flux and accelerating ion transport kinetics via zincophilic covalent organic framework interlayer for stable Zn metal anode. *Chemical Engineering Journal* **2024,** *485*, 149813.
21. Li, X.; Chu, Y.; Lu, S.; Chen, L.; Su, L.; Lu, F.; Chen, Z.; Gao, X., Fluorinated Zn-porphyrin covalent organic frameworks with optimized hydrophobic/hydrophilic balance towards stable Zn anodes. *Chemical Engineering Journal* **2025,** *505*, 159182.
22. Li, B.; Ruan, P. C.; Xu, X. Y.; He, Z. X.; Zhu, X. Y.; Pan, L.; Peng, Z. Y.; Liu, Y. Y.; Zhou, P.; Lu, B. A.; Dai, L.; Zhou, J., Covalent Organic Framework with 3D Ordered Channel and Multi-Functional Groups Endows Zn Anode with Superior Stability. *Nano-Micro Letters* **2024,** *16* (1), 76.
23. Li, D.; Long, J.; Liu, X.; Chen, X.; Li, Z.; Lei, G., Simple MOF Composite Coating-Modified Zinc Metal Anode for Aqueous Zinc-Ion Batteries. *Energy & Fuels* **2025,** *39* (18), 8742-8752.
24. Wang, Z. A.; Wang, P.; Zhang, J. X.; Yang, X. Y.; Wu, X. L.; Duan, W.; Yue, Y.; Xie, J.; Liu, Y. P.; Tian, H. J., Superhydrophobic metal-organic framework layers as multifunctional ion-conducting interfaces for ultra-stable Zn anodes. *Journal of Power Sources* **2024,** *622*, 235364.
25. Zhao, Z. H.; Zhang, H. D.; Shi, X. W.; Zhang, Y.; Tang, C.; Zhao, H. T.; Liu, J. M.; Wang, G. L.; Li, L., Zincophilic Metal-Organic-Framework Interface Mitigating Dendrite Growth for Highly Reversible Zinc Metal Batteries. *Small* **2024,** *20* (6), 2304723.
26. Zhang, W.; Qi, W.; Yang, K.; Hu, Y.; Jiang, F.; Liu, W.; Du, L.; Yan, Z.; Sun, J., Boosting tough metal Zn anode by MOF layer for high-performance zinc-ion batteries. *Energy Storage Materials* **2024,** *71*, 103616.
27. Gopalakrishnan, M.; Hlaing, M. T.; Kulandaivel, T.; Kao-ian, W.; Etesami, M.; Liu, W.-R.; Nguyen, M. T.; Yonezawa, T.; Limphirat, W.; Kheawhom, S., Tunable N-doped carbon dots/SnO_2 interface as a stable artificial solid electrolyte interphase for high-performance aqueous zinc-ion batteries. *Journal of Alloys and Compounds* **2025,** *1013*, 178521.
28. Gong, S. H.; Lim, H. J.; Lee, J. H.; Yoo, Y.; Yu, S.; Lim, H.-D.; Jung, H. W.; Ko, J. S.; Kim, I. S.; Kim, H.-S., Electrochemical assessment of highly reversible SnO_2–coated Zn metal anodes prepared via atomic layer deposition for aqueous Zn-ion batteries. *Applied Surface Science* **2023,** *611*, 155633.